



저작자표시-비영리 2.0 대한민국

이용자는 아래의 조건을 따르는 경우에 한하여 자유롭게

- 이 저작물을 복제, 배포, 전송, 전시, 공연 및 방송할 수 있습니다.
- 이차적 저작물을 작성할 수 있습니다.

다음과 같은 조건을 따라야 합니다:



저작자표시. 귀하는 원저작자를 표시하여야 합니다.



비영리. 귀하는 이 저작물을 영리 목적으로 이용할 수 없습니다.

- 귀하는, 이 저작물의 재이용이나 배포의 경우, 이 저작물에 적용된 이용허락조건을 명확하게 나타내어야 합니다.
- 저작권자로부터 별도의 허가를 받으면 이러한 조건들은 적용되지 않습니다.

저작권법에 따른 이용자의 권리는 위의 내용에 의하여 영향을 받지 않습니다.

이것은 [이용허락규약\(Legal Code\)](#)을 이해하기 쉽게 요약한 것입니다.

[Disclaimer](#)

Abstract

The Effect of Combined Treatment with SRC Tyrosine Kinase Inhibitor, PP2 and Temozolomide on Malignant Glioma Cells *in vitro* and *in vivo*

Keun-Yong Eom

Radiation Oncology

The Graduate School

Seoul National University

Introduction: Overexpression of SRC tyrosine kinase of glioblastoma is associated with aggressiveness of tumors and poor treatment outcomes. We surveyed whether combined treatment of temozolomide (TMZ) and SRC tyrosine kinase inhibitor (TKI), PP2 would inhibit growth and invasion of glioma cells and thus, improve therapeutic efficacy of radiotherapy using *in vitro* clonogenic assays and an *in vivo* human brain tumor xenograft model in nude mice.

Methods & Materials: The effect of the SRC TKI, PP2 (10 μ M) on radiosensitivity of U251 and T98G cells with or without TMZ (25 μ M) using *in vitro* clonogenic assays was investigated. It was also examined whether pretreatment with PP2 before radiotherapy inhibits DNA DSBs repair by measuring γ H2AX foci formation 6 h after radiotherapy. The effect of PP2 on migration and invasion ability of U251 cells were evaluated using modified Boyden chamber assay and wound healing assay. Vasculogenic mimicry (VM) formation assay was also performed. Western blot analyses were performed to measure the protein expression including E-cadherin, MMP2, EphA2, and VEGF after PP2 treatment. In *in vivo* human brain tumor xenograft model in nude mice, 3×10^5 U251 cells were implanted to the thalamus and PP2 (10mg/kg) was treated with or without TMZ (50 mg/kg) before, during and after whole brain radiotherapy of 9 Gy in 3 fractions. Bioluminescence images using pGL4 luciferase reporter vector were taken after inhibitor treatment to measure *in vivo* tumor volume.

Immunohistochemical stains including VEGF, CD31, EphA2, and HIF1a was performed on brain tumors.

Results: Pretreatment with PP2 increased cytotoxicity and decreased surviving fraction of U251 cells after radiotherapy without obvious cytotoxic effects on normal human astrocytes. The sensitizer enhancement ratio at a surviving fraction of 0.5 ($SER_{0.5}$) for PP2, TMZ, and PP2 plus TMZ was 1.15, 1.41, and 1.54 in U251 cells, and 1.16, 1.26, and 1.38 in T98G cells, respectively. Invasion and migration ability of U251 cells were compromised by PP2 treatment. The relative migration of inhibitor-treated cells relative to cells treated with radiotherapy alone was 0.993 ± 0.131 ($p = 0.465$), 0.252 ± 0.078 ($p < 0.001$), and 0.200 ± 0.066 ($p < 0.001$) for TMZ, PP2, and TMZ plus PP2, respectively. The relative invasion ability of inhibitor-treated cells relative to cells treated with radiotherapy alone was 0.992 ± 0.122 ($p = 0.461$), 0.257 ± 0.050 ($p < 0.001$), and 0.116 ± 0.010 ($p < 0.001$) for TMZ, PP2, and TMZ plus PP2, respectively. VM formation was also suppressed by PP2. After PP2 treatment, overexpression of E-cadherin, and suppression of MMP2, VEGF, and EphA2 were observed. PP2 treatment combined with TMZ resulted in increased accumulation of γ H2AX foci, indicating delayed DNA damage repair.

In a human brain tumor xenograft model, combined treatment with PP2 and TMZ showed best tumor volume decrease, but the difference from TMZ alone was not statistically significant. The expression of VEGF and CD31 were down-regulated in PP2-treated tumors relative to RT alone or RT plus TMZ treated tumors, suggesting that PP2 may suppress angiogenesis in *in vivo* tumor as well as in *in vitro* cells. The expression of EphA2 and HIF1a of *in vivo* brain tumors were not influenced by PP2 treatment.

Conclusions: These results show that SRC tyrosine kinase inhibition leads to additive cytotoxicity of radiotherapy in malignant glioma cells and this effect was independent of MGMT promoter methylation status. PP2 also decreased invasion, migration, and VM formation of U251 cells. PP2 suppressed VEGF and CD31 expression and thus, showed anti-angiogenic potential in *in vivo* model using U251 cells. These results provide evidences for the combination therapy of TMZ and SRC TKI, PP2 on malignant glioma cells and present a feasible strategy to improve the therapeutic outcomes.

Keywords: SRC tyrosine kinase inhibitor, PP2, glioblastoma, malignant glioma, combined

treatment, radiotherapy

Student Number: 2008-30529

Table of Contents

| | |
|-----------------------------|----|
| Abstract | i |
| Table of contents | iv |
| List of figures | v |
| Introduction | 1 |
| Materials and Methods | 3 |
| Results | 8 |
| Discussion | 17 |
| References | 20 |

List of Figures

| | |
|--|----|
| Figure 1. Study scheme of <i>in vivo</i> human brain tumor model..... | 6 |
| Figure 2. Clonogenic assays of U251 and T98G cells after treating PP2, temozolomide (TMZ), or both..... | 9 |
| Figure 3. Western blot analysis of U251 cells after inhibitor treatment..... | 10 |
| Figure 4. Representative images of γH2AX foci formation in U251 cells | 11 |
| Figure 5. Representative images of (A) modified Boyden chamber assay, (B) wound healing assay, and (C) vasculogenic mimicry formation assay..... | 12 |
| Figure 6. The surviving fraction at 2 Gy (SF2) of X-ray in normal human astrocytes..... | 13 |
| Figure 7. Representative bioluminescence images of human brain tumor xenograft in nude mice..... | 14 |
| Figure 8. Immunohistochemical stains of <i>in vivo</i> human brain tumors in nude mice..... | 16 |

Introduction

Malignant glioma is the most common neoplasm arising in the central neural system in adults and one of the most aggressive human tumors, with a grave prognosis. Among this disease category, glioblastoma (GBM) shows the worst prognosis despite aggressive multimodality treatment. Several molecular markers are being used in clinical diagnosis of GBM and give prognostic informations of each patient. (1, 2) Among them, methylation of the O6-methylguanine-DNA methyltransferase (*MGMT*) promoter gene is predictive for the outcomes of GBM and the therapeutic efficacy of TMZ depends on expression of *MGMT* gene. Methylation of this promoter is associated with *MGMT* gene silencing and improved prognosis. With the advent of temozolomide (TMZ), the standard treatment for GBM has become maximal safe resection followed by concurrent chemoradiotherapy with TMZ and adjuvant TMZ. Nonetheless, the actuarial survival rate of patients with GBM remains disappointing because *MGMT* promoter methylation is present in only 45% of patients, and even in patients with *MGMT* promoter methylation the survival rate at 2 years is only 46% at best despite aggressive treatment. (3) Thus, it is essential to improve therapeutic efficacy without considerable toxicity to overcome dismal prognosis of GBM.

Several molecular targets are undergoing extensive investigation to meet these needs and inhibition of a target molecule or signaling pathways with a single agent was successful in some cancers, but in others often resulted in the failure because of development of treatment resistance. As a solution to the problem, dual inhibition of a signaling pathway, combining a targeting agent with chemotherapeutic agents, or combining targeting agents abrogating different pathways has been tried and showed promising results in some tumors. (4-7)

As most of the treatment failure in GBM occurs in central area (8), inhibiting invasion or migration of GBM can be one of the promising strategies to improve treatment outcomes. In this regard, because SRC tyrosine kinase regulates actin dynamics and invasion of malignant glial cells (9), SRC tyrosine kinase is one of the most promising candidate. SRC tyrosine kinase is an enzyme encoded by the *SRC* gene that belongs to a family of non-receptor tyrosine kinases. (10) SRC tyrosine kinase interacts with many intracellular proteins including growth factor receptors, integrins, and Eph kinase, and mediates signals from the extracellular matrix. Elevated SRC tyrosine kinase activity of GBM cells relative to normal brain cells has been

shown in previous reports (11, 12) and an inhibitory effect on cell invasion and migration by SRC tyrosine kinase inhibitors (TKI) in GBM cell lines has been demonstrated (12-15). In regard to radiotherapy, ionizing radiation enhances invasion of glioma cells through SRC/epidermal growth factor receptor-mediated p38/AKT and phosphatidylinositol 3-kinase/AKT signaling pathways.(16) In addition, SRC TKI AZD0530 blocks invasion and may act as a radiosensitizer in lung cancer cells (17) and SRC TKI Su6656 enhances antiangiogenic effect of irradiation.(18)

Therefore, we investigated whether combined treatment of TMZ and SRC TKI, PP2 would inhibit migration and growth of glioma cells and thus, improve therapeutic effect of radiotherapy using *in vitro* clonogenic assays and an *in vivo* human brain tumor xenograft model in nude mice.

Materials and Methods

Cell lines and culture conditions

Human glioma cell lines U251 and T98G purchased from the American Tissue Culture Collection (Rockville, MD, USA) were authenticated by the company's routine Cell Biology Program and used within 6 months of receipt. Cells were maintained and cultured in Dulbecco's Modified Eagle Medium (DMEM; Lonza, MD, USA) media containing 10% fetal bovine serum (FBS; Gibco, NY, USA) at 37°C in 5% CO₂ using standard techniques.

Inhibitors

The SRC TKI PP2 (4-amino-5-(4-chlorophenyl)-7-(*t*-butyl)pyrazolo[3,4-*d*]pyrimidine) is commonly used in cancer research as a selective inhibitor of SRC-family kinases such as Lck, Fyn, and Hck. (19) PP2 (Calbiochem, Darmstadt, Germany) was prepared as a concentrated stock solution in dimethyl sulfoxide (DMSO; Sigma-Aldrich, St. Louis, MO, USA), stored at -20°C, and diluted in culture medium at the time of use. TMZ (Schering-Plough, Kenilworth, NJ, USA) was prepared by dissolving in 10 mM sodium chloride.

Clonogenic assay

Cancer cells were seeded in 6-well plates. On the first day of treatment, the medium was replaced with DMEM lacking FBS and containing vehicle control or 10 µM PP2, with or without 25 µM TMZ. After 24 h, the medium was replaced with DMEM containing 10% FBS. Control cells were treated with medium containing the same concentration of DMSO.

After exposure to inhibitors, cells were irradiated with 6 megavoltage X-rays from a linear accelerator (Clinac 21EX; Varian Medical Systems, Palo Alto, CA, USA) at a dose rate of 0.6Gy/min and incubated for 14 to 21 days for colony formation. Colonies were fixed with methanol and stained with 0.5% crystal violet. The number of colonies containing at least 50 cells was counted and the surviving fraction was calculated. Survival data were fitted to a linear-quadratic model using Kaleidagraph version 3.51 (Synergy Software, Reading, PA, USA). Each point on the survival curves represents the mean surviving fraction from at least three dishes. Sensitizer enhancement ratios (SER) of human glioma cells were calculated at 50% or 5% cell

survival by dividing the radiation dose from the survival curve of radiation alone by the corresponding dose from the survival curve of inhibitor treatment.

γ H2AX foci formation assay

Cells were grown and treated on chamber slides. After treating inhibitors for 6 h, the coverslips were rinsed and the cells were fixed in 4% paraformaldehyde, permeabilized in methanol for 20 minutes, and blocked in PBS containing 2% bovine serum albumin for 1 h. Slides were incubated overnight with primary antibody against γ H2AX (Cell Signaling Technology, Danvers, MA, USA), followed by incubation with secondary Alexa Fluor 488–conjugated donkey anti-goat antibody (Molecular Probes, Eugene, Oregon, USA) for 1 h. Slides were treated with 1 μ g/mL 4',6-Diamidino-2-phenylindole for 5 minutes to counterstain nuclei and examined on an Axio Scope A1 Microscope.

Modified Boyden chamber assay

Cell migration was measured using a Transwell system (Corning, Rochester, NY, USA) that allows cells to migrate through 8- μ m pores in polycarbonate membranes. Inserts containing cancer cells were incubated in 24-well plates (Corning) in serum-free medium and cells were harvested by trypsinization. An aliquot of 10^4 cells was added to the upper chamber and DMEM was placed in the lower chamber of Transwells, and incubated for 24 h. The inserts were fixed in methanol, stained with 1% crystal violet, and three representative fields were photomicrographed.

Wound healing assay

Cells were cultured until confluent in 6-well plates (SonicSeal Slide; Nalge Nunc, Rochester, NY, USA) and starved for 24 h. Each well was divided into a 2×3 grid. A linear wound was made in each hemisphere of the well using a 1-mL pipette tip and the medium was replaced with starvation medium. After 24 h, images were obtained at the intersections of the linear cell wound and each grid line. Migration rate was estimated from the distance that the cells moved, as determined microscopically.

Vasculogenic mimicry (VM) formation assay

VM formation assay was performed using a commercial Matrigel assay kit (BD Biosciences, le Pont de Claix, France). ECM Matrigel (200 μ L) was placed in 48-well tissue culture plates and incubated at 37°C for 2 h. Cells were treated with TMZ (25 μ M) with or without PP2 (10 μ M), and seeded onto the coated plate. After incubation for 24 h, VM formation was assessed using an inverted microscope.

Western blot analysis

Cells were washed twice with cold PBS, scraped in PBS, and resuspended in lysis buffer (iNtRON Biotechnology, Seoul, Korea). Equal amounts of protein solubilized by sonication and separated by sodium dodecyl sulfate polyacrylamide gel electrophoresis (SDS-PAGE) were electroblotted onto polyvinylidene difluoride membranes (Millipore Corp., Bedford, MA, USA). Membranes were blocked in PBS containing 0.1% Tween 20 and 5% powdered milk and probed with primary antibodies against p-SRC (Thy416), p-EGFR (Tyr1068), p-AKT (Ser473), p-ERK (Tyr202/204), E-cadherin, matrix metalloproteinase 2 (MMP2), and Ephrin type-A receptor 2 (EphA2) at 1:1000 dilutions. Primary antibodies against vascular endothelial growth factor (VEGF) and β -actin (Santa Cruz Biotechnology, Santa Cruz, CA, USA) were used at a dilution of 1:500 and 1:1000, respectively. Membranes were washed and incubated with peroxidase-conjugated goat anti-rabbit or anti-mouse IgG secondary antibody (Jackson ImmunoResearch Laboratories, West Grove, PA, USA) at a dilution of 1:2500.

***In vivo* imaging of a human brain tumor model in nude mice**

U251 cells (3×10^5 cells) were injected intracranially using a 26-G needle attached to a Hamilton syringe with freehand technique over 1 minute. On day 7 of cell implantation, the pGL4 luciferase reporter vector (Promega, Madison, Wisconsin, USA) 150 mg/Kg was injected intraperitoneally and after 15 minutes, mice were anesthetized with 1-2% isoflurane as usual. *In vivo* bioluminescence images were obtained using the IVIS Lumina II (Xenogen, Alameda, CA, USA) to identify intracranial implants.

Mice were randomly assigned to the experimental or control group and were treated over 3 weeks as follows: (1) radiotherapy alone group: PBS was injected intraperitoneally on days 8,

10, 12, 15, 17, 19, 22, 24, and 26; (2) inhibitor treatment group: PP2 (10 mg/kg) was injected intraperitoneally and TMZ (50 mg/kg) was given orally per day on the same treatment days as the control group. (Figure 1)

Two hours after inhibitor treatment, external radiotherapy was performed with a 6 MeV electron beam (Clinac 21EX) to cover the whole brain of the mouse. A total of 9 Gy was delivered with a daily dose of 3 Gy on days 15, 17, and 19. Bioluminescence images were obtained 2 weeks after radiotherapy as described. Mice were sacrificed on day 35 according to the IACUC protocol unless they became symptomatic from the intracranial tumor burden.

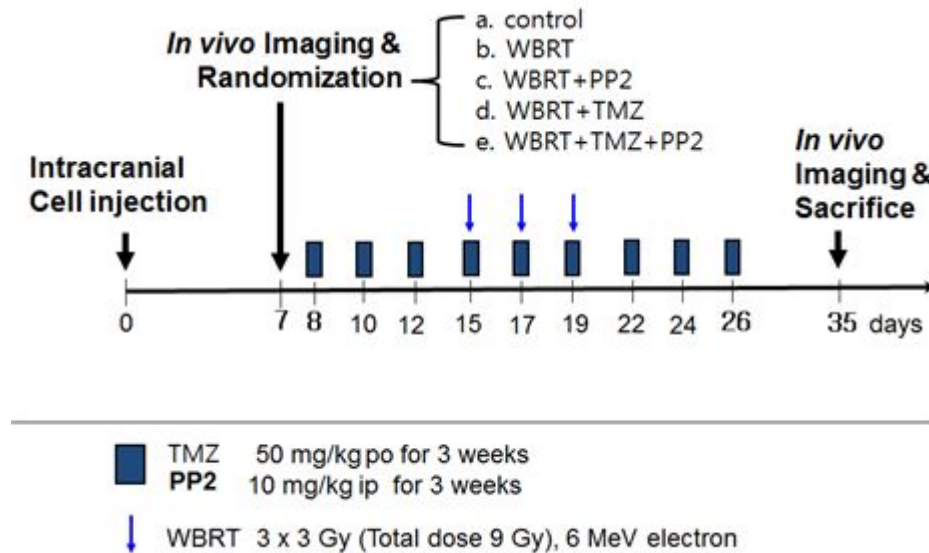


Figure 1. Study scheme of *in vivo* human brain tumor model. Abbreviations: RT, Radiotherapy; WBRT, whole brain radiotherapy; and TMZ, temozolomide.

Cryosection and immunohistochemical stains of harvested tumors

Fresh brain tumors were frozen in OCT (Tissue-Tek, Miles, IN, USA) in a suitable tissue mold at -20°C in cryostat. Cryosections with 5-10 µm thickness were performed. Tumor sections were mounted on gelatin-coated histological slides and dried in room air for 30 minutes. Tissues were fixed with 50 µL of ice-cold Fixation Buffer for 20 minutes at -20°C, and blocked in PBS containing 2% bovine serum albumin for 1 h. Slides were incubated overnight with primary antibody against VEGF, CD31, EphA2, and HIF1a. (Cell Signaling Technology), followed by

incubation with secondary Alexa Fluor 488–conjugated donkey anti-goat antibody (Molecular Probes, Eugene, Oregon, USA) for 1 h. Slides were treated with 1 µg/mL 4',6-Diamidino-2-phenylindole for 5 minutes to counterstain nuclei and examined on an Axio Scope A1 Microscope. Images were captured and acquired using AxioCam MRc5 and acquisition software AxioVision v.4.4 (Carl Zeiss, Gottingen, Germany).

Statistical analysis

The statistical analysis using IBM SPSS program, version 20 was performed. Student's t-test was used to analyze statistical significance as applicable. P value less than 0.05 was considered statistically significant.

Results

Radiosensitizing effect of PP2 in U251 and T98G cells

First clonogenic assays were performed to evaluate the radiosensitizing effect of PP2 (Figure 1). Combination of PP2 with TMZ showed an additive cytotoxic effect in U251 and T98G cells. The SER at a surviving fraction of 0.5 (SER_{0.5}) for PP2, TMZ, and PP2 plus TMZ was 1.15, 1.41, and 1.54 in U251 cells, and 1.16, 1.26, and 1.38 in T98G cells, respectively. U251 cells, which have a high proportion of methylated MGMT, showed a higher degree of radiosensitization by TMZ. In contrast, T98G cells with a low proportion of methylated MGMT showed less radiosensitization by TMZ. PP2 induced additional cytotoxic effect on glioma cells irrespective of MGMT promoter methylation status.

Impairment of DNA damage repair following irradiation

Since DNA double strand breaks (DSBs) induced by radiotherapy are responsible for cell death, repair of DSBs is crucial for cellular survival. It was examined whether pretreatment with SRC TKI before radiotherapy inhibits DNA DSBs repair by measuring γ H2AX foci formation 6 h after radiotherapy. Pretreatment with PP2 combined with TMZ resulted in increased accumulation of γ H2AX foci, indicating PP2 induced delayed repair of DNA DSBs. (Figure 3)

PP2 inhibits glioma cell invasion, migration, and VM formation

Second, whether PP2 can inhibit invasion and migration of U251 cells was evaluated. In a modified Boyden chamber assay, cell migration was inhibited by PP2, with or without TMZ (Figure 4A). The number of migrating cells in the control was not statistically different from that of TMZ-treated cells ($p = 0.468$). However, pretreatment with PP2 markedly suppressed migration of U251 cells. The relative migration of inhibitor-treated cells relative to cells treated with radiotherapy alone was 0.993 ± 0.131 ($p = 0.465$), 0.252 ± 0.078 ($p < 0.001$), and 0.200 ± 0.066 ($p < 0.001$) for TMZ, PP2, and TMZ plus PP2, respectively.

U251

T98G

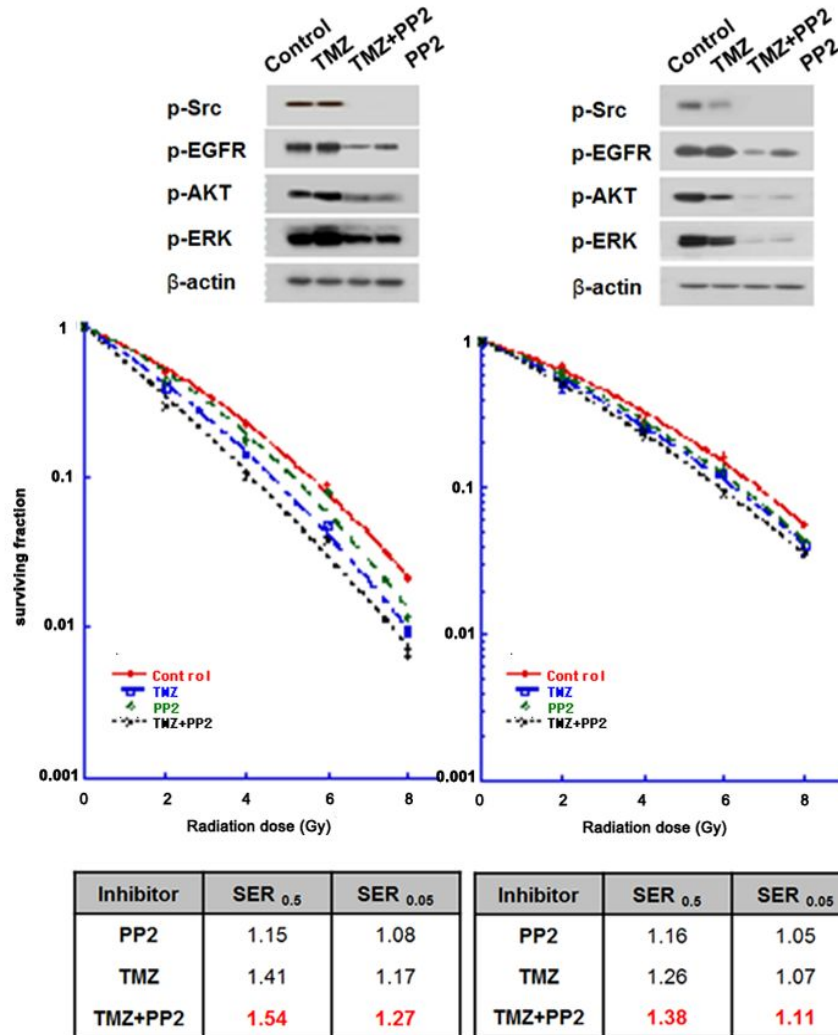


Figure 2. Clonogenic assays of U251 and T98G cells after treating PP2, temozolomide (TMZ), or both. Cell surviving curves after treating PP2 (10uM), TMZ (25uM), or both were generated. The points indicate the mean surviving fractions at each dose level (\pm SE). The lines are fitted to linear-quadratic equations. An addition of PP2 to TMZ showed an additive cytotoxic effect both in U251 and T98G cells. Sensitizer enhancement ratios (SER) were calculated at 50% or 5% cell survival by dividing radiation dose from the radiation-only surviving curve with the corresponding dose from inhibitor-treated surviving curve. PP2 induced radiosensitization in U251 and T98G cells irrespective of MGMT promoter methylation.

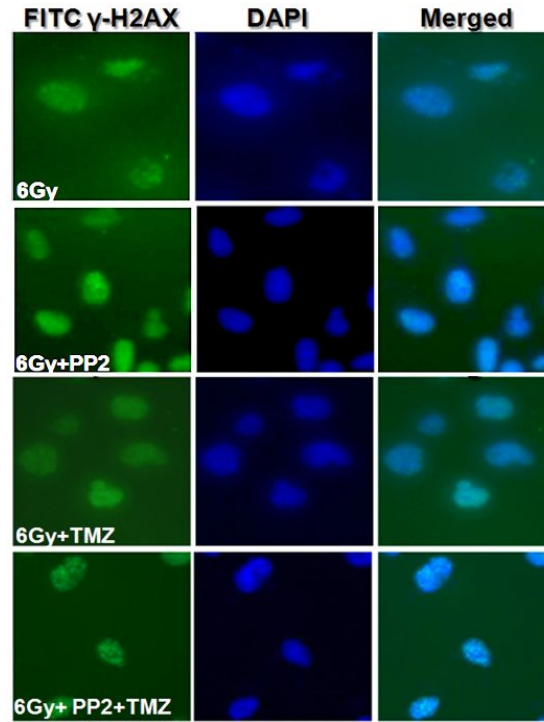


Figure 3. Representative images of γ H2AX foci formation in U251 cells. γ H2AX foci formation was measured in U251 cells after treating PP2 (10uM), temozolomide (TMZ, 25uM), or both. The nuclei stained by DAPI are shown in blue, while the γ H2AX foci stained by FITC are shown in green. Increased accumulation of γ H2AX foci after treating PP2 and TMZ was confirmed by indirect immunofluorescence 6 h after radiotherapy (6 Gy), indicating delayed DNA double strand breakage repair.

In a wound healing assay, the invasion ability of U251 cells was measured 24 h after scratching (Figure 4B). PP2 inhibited invasion of U251 cells, whereas TMZ did not. The relative invasion ability of inhibitor-treated cells compared with cells treated with radiotherapy alone was 0.992 ± 0.122 ($p = 0.461$), 0.257 ± 0.050 ($p < 0.001$), and 0.116 ± 0.010 ($p < 0.001$) for TMZ, PP2, and TMZ plus PP2, respectively.

As malignant gliomas have been reported to exhibit VM, which is related to aggressiveness or mesenchymal transition of cancer cells and related to poor survival, we investigated the effect of PP2 on vascular formation using a VM formation assay. As shown in Figure 4C, pretreating PP2, with or without TMZ, inhibited VM formation.

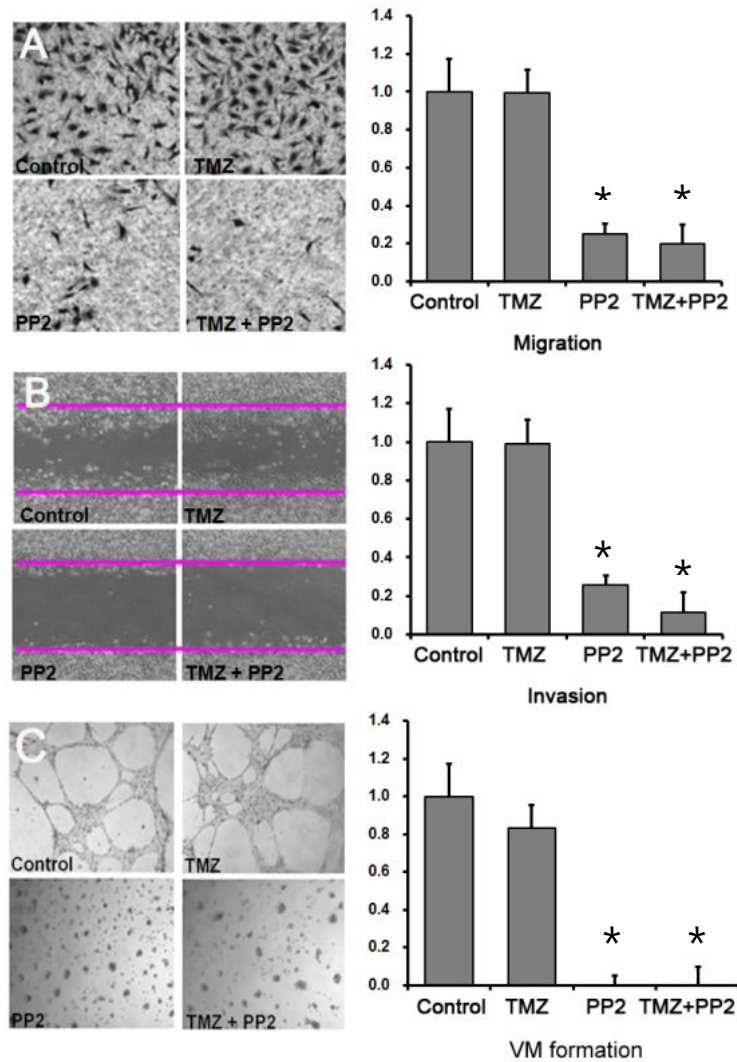


Figure 4. Representative images of (A) modified Boyden chamber assay, (B) wound healing assay, and (C) vasculogenic mimicry formation assay. (A) U251 cells were treated with PP2 (10uM), temozolomide (TMZ; 25 uM), or both for 24 h, and cell invasion was measured using a Transwell system with 8- μ m pores in polycarbonate membranes. Results are expressed as a ratio of radiotherapy alone (control). (B) U251 cells were grown to confluence in 6-well plates and then starved for 24 h. A linear scratch was made in each hemisphere of the well with 1mL pipette tip. Images were taken of the intersections of linear cell wound and each grid line. (C) 200 μ L ECM Matrigel was dropped in 48-well tissue culture plates and then incubated at 37°C for 2 h. Column: Mean of three independent experiments. Bar: SE. Asterisk: statistical significance of $p < 0.05$ when compared with control.

Changes in protein expression following PP2 and TMZ treatment

To investigate changes in protein expression related to invasion or migration of U251 cells after treating inhibitors, proteins related to cell adhesion or vascular proliferation, including E-cadherin, MMP2, EphA2, and VEGF, were evaluated using Western blot analysis. As shown in Figure 5, pretreatment with TMZ did not alter the expression of these proteins, whereas PP2 treatment resulted in suppression of MMP2, EphA2, and VEGF and overexpression of E-cadherin in U251 cells.

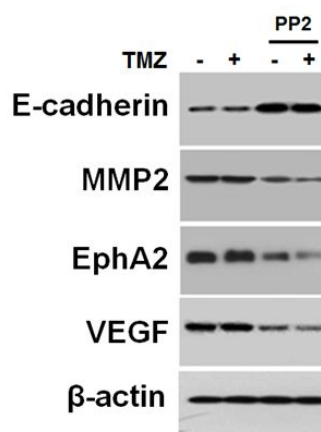


Figure 5. (A) Western blot analysis of U251 cells after treating inhibitors. After PP2 (10 μ M) treatment, E-cadherin was overexpressed, while expression of MMP2, EphA2, and VEGF were suppressed.

Effect of PP2 on normal human astrocytes (NHAs)

To assess whether SRC TKI has a cytotoxic effect on NHAs in the concentration of 10 μ M, the SF2 of NHAs after treating PP2, TMZ, or both, compared to control (Figure 6) was examined. PP2 did not decrease SF2 compared with control, suggesting that SRC TKI does not affect the viability of NHAs. SF2 of PP2 plus TMZ was not different from that of TMZ alone.

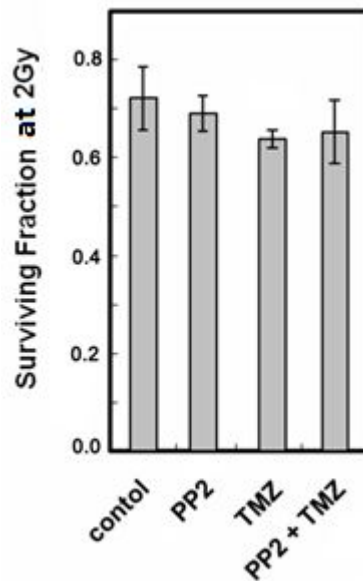


Figure 6. The surviving fraction at 2 Gy (SF2) of X-ray in normal human astrocytes. SF2 was measured after treating PP2 (10 μ M), temozolomide (TMZ; 25 μ M), or both. The points indicate the mean surviving fractions at each dose level (\pm SE). Column: Mean of three independent experiments. Bar: SE.

***In vivo* tumor response after PP2 treatment and radiotherapy**

As shown Figure 2, *in vitro* experiments revealed that pretreatment with PP2 induced additional cell death of U251 cells with or without TMZ. We investigated whether adding PP2 to TMZ would result in better local control of brain gliomas using a human brain tumor xenograft model in nude mice. Radiotherapy alone induced tumor shrinkage, but failed to achieve complete remission (Figure 7A). Pretreatment of TMZ exhibited a better tumor response than radiotherapy alone, and PP2 plus TMZ led to best visual response of tumors, indicating an additional radiosensitizing effect of PP2.

As semi-quantitative analyses, the area and mean intensity of luminescence was measured and compared to each other. There was a significant difference between control and inhibitor treated groups in area of luminescence ($P = 0.025$, 0.004 and 0.004 for PP2, TMZ, and PP2 plus TMZ, respectively). Figure 7B shows a trend that combination of PP2 and TMZ results in a smaller area of luminescence than TMZ or PP2 alone, but it was not statistically significant.

Temozolomide-treated groups had smaller mean intensity than control or radiotherapy alone (Figure 7C). However, the difference between TMZ and PP2 plus TMZ was not significant.

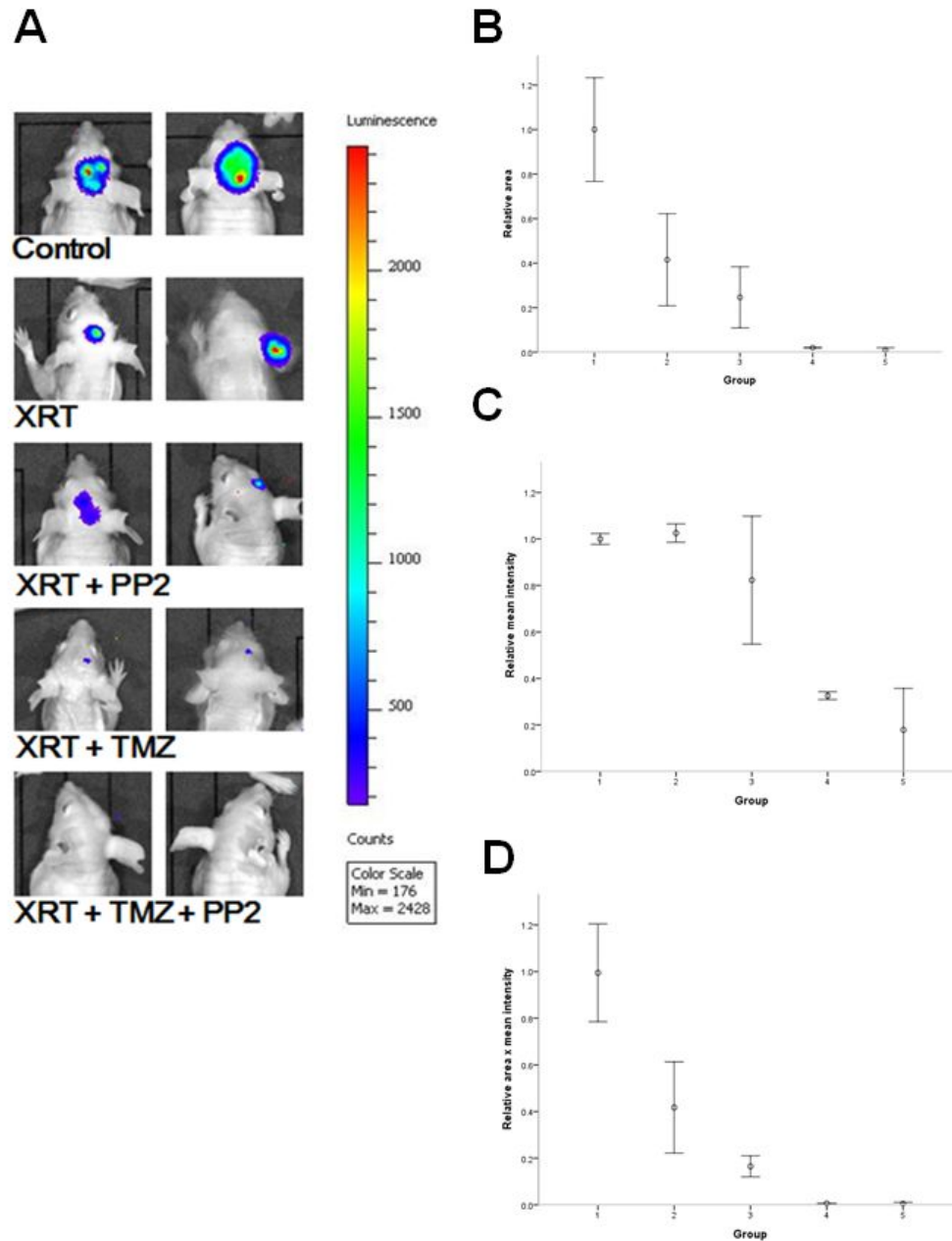


Figure 7. Representative bioluminescence images (A) of human brain tumor xenograft in nude mice. U251 cells were injected orthotopically into thalamic area using a 26G needle with syringe. Bioluminescence images were obtained 7 days after injection, and then randomly assigned to control or experimental groups as follows: control (group 1), XRT (group2),

XRT+PP2 (group 3), XRT+TMZ (group 4), and XRT+TMZ+PP2 (group 5), respectively. Tumor responses in TMZ (50mg/kg) treatment group were better than those of radiotherapy alone, and PP2 (10mg/kg) plus TMZ induced non-visualization of brain tumors, indicating radiosensitizing effect of PP2 in malignant gliomas. In semi-quantitative analyses of (B) relative luminescence area, combination of PP2 and TMZ resulted in a smaller area of luminescence than TMZ or PP2 alone, but it was not statistically significant. In (C) relative mean intensity, combination of TMZ and PP2 showed decrease of relative mean luminescence intensity. (D) Relative area x mean intensity of luminescence of brain tumors. Bar: SE, XRT: radiotherapy, TMZ: temozoloide.

Immunohistochemical stains of brain tumors

To elucidate changes of protein expression induced by PP2 treatment in *in vivo* model, immunohistochemical stains with antibodies against VEGF, CD31, EphA2, and HIF1a were performed. As shown in Figure 8, expression of VEGF and CD31 were down-regulated in PP2-treated tumors relative to RT alone or RT plus TMZ tumors, suggesting that PP2 may suppress angiogenesis in *in vivo* tumor as well as in *in vitro* cells. Expression of EphA2 and HIF1a were not influenced by PP2 treatment in *in vivo* tumors.

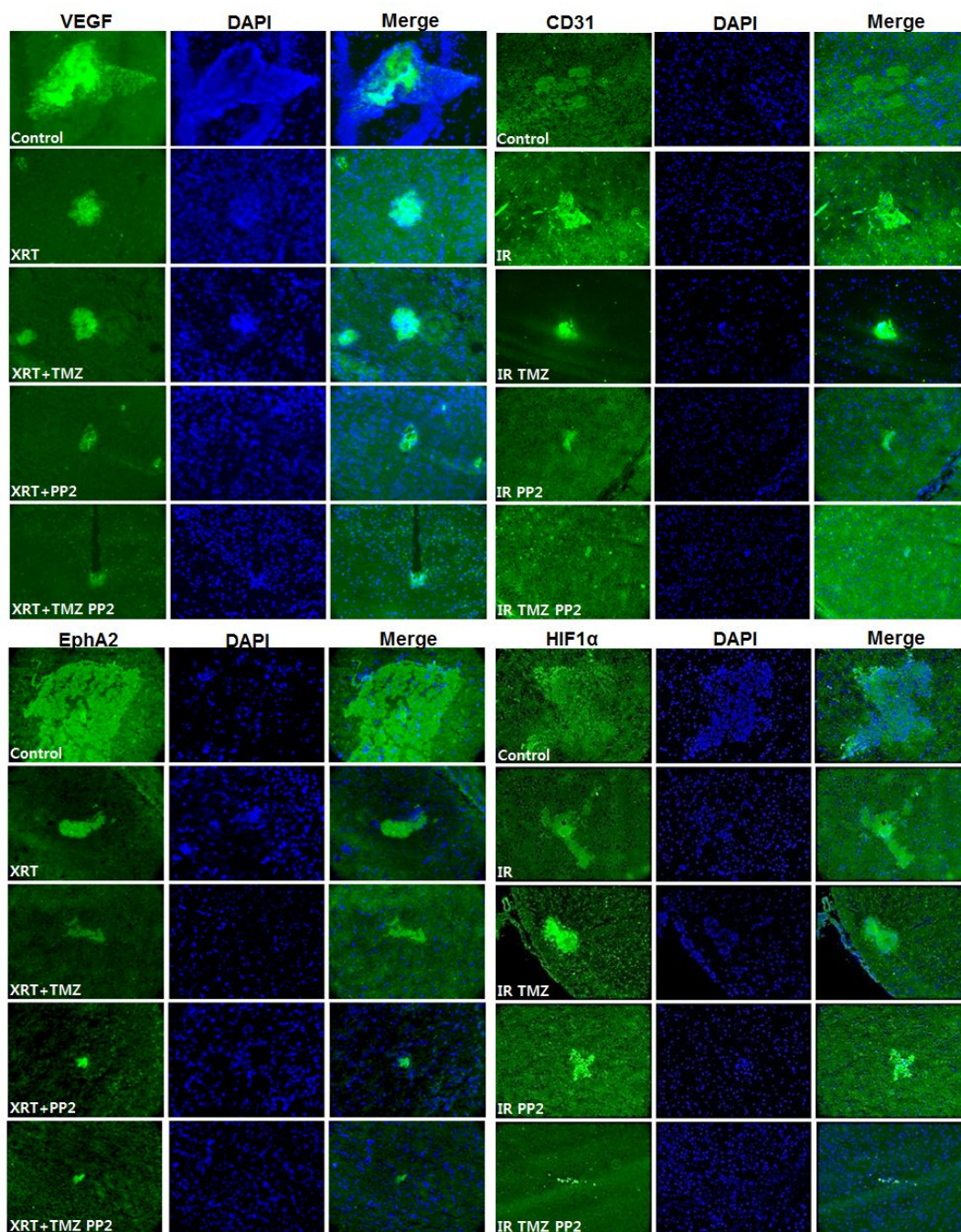


Figure 8. Immunohistochemical stains of in vivo human brain tumors in nude mice.

Imunohistochemical stains with antibodies against VEGF, CD31, EphA2, and HIF1a were performed. The expression of VEGF and CD31 were down-regulated in PP2-treated tumors relative to those with RT alone or RT plus TMZ tumors, which suggests that PP2 may suppress angiogenesis in *in vivo* tumor as well as in *in vitro* cells. Expression of EphA2 and HIF1a were not influenced by PP2 treatment in *in vivo* tumors.

Discussion

In this study, we evaluated the effect of combined therapy using TMZ and SRC TKI PP2 on malignant glioma cells using *in vitro* and *in vivo* experiments. In *in vitro* experiments, our data demonstrated that pretreating PP2 shows small, but additive cytotoxic effect and this effect is irrespective of MGMT promoter methylation status of glioma cells when combined with radiotherapy, which suggests SRC tyrosine kinase can be a novel target for GBM treatment. PP2 did not increase death of NHAs in the same concentration. As shown in Figure 4, pretreating PP2 demonstrated delayed repair of DNA DSBs induced by radiotherapy.

Infiltrative growth is a key characteristic of malignant gliomas, which hinders complete surgical removal of gliomas and often results in local recurrence despite aggressive treatment including surgery and chemoradiotherapy. Suppressing invasion and/or migration of glioma cells can be one of possible strategies to overcome dismal prognosis of GBM. In modified Boyden chamber assay and wound healing assay which measure invasion and migration ability of cancer cells, PP2 inhibited both invasion and migration of U251 cells with statistical significance (Figure 4). It is generally accepted that loss of E-cadherin, which may affect cell-to-cell adhesion and relate to invasive property, is a fundamental event in epithelial-mesenchymal transition (EMT). In this study, pretreating PP2 resulted in overexpression of E-cadherin and suppression of MMP2, and EphA2 in U251 cells (Figure 5). These suggest that PP2 inhibits invasion and migration ability of U251 cells, affecting adhesion molecules such as E-cadherin. Taken together, it is clear that PP2 suppresses invasion and/or migration ability of glioma cells. These results are consistent with other studies, in which SRC regulates actin dynamics and invasion of malignant glial cells. (9, 20)

Neovascularization is essential for the rapid growth of tumors and is crucial characteristic of malignant gliomas. Some targeting agents, such as Bevacizumab, a monoclonal antibody to VEGF-A, aim to suppress neovascularization of tumors and as a consequence, inhibit tumor growth. (21) In clinical practice, Bevacizumab is being applied as a second line drug to salvage recurrent GBM.(22) In this study, we measured the effect of PP2 on the expression of VEGF using Western blot analysis and tested VM formation of U251 cells. It was revealed that the expression of VEGF was down-regulated and VM formation is excellently inhibited by

pretreatment with PP2 in U251 cells, which suggests SRC TKI may inhibit neovascularization of malignant gliomas. In *in vivo* experiment using nude mice, human xenograft brain tumor model, the expression of VEGF and CD31 in implanted brain tumors was also suppressed as shown in Figure 8. These results strongly suggest an anti-angiogenic potential of SRC TKI in malignant gliomas. Moreover, recent study suggests that suppressing SRC family kinase (SFK) signaling can inhibit Bevacizumab-induced GBM cell invasion, suggesting a possible strategy to overcome treatment resistance of GBM. (23)

Suppression of matrix metalloproteinase 2 (MMP2) might play a role in the restoration of radiation sensitivity in glioma cells. MMP2 is implicated in the invasiveness of glioma cells, which convert the pro-form of MMP2 into the active form through the urokinase-type plasminogen activator-plasmin cascade. (24) Ionizing radiation enhances MMP2 secretion and facilitates invasion of glioma cells through SRC/EGFR-mediated PI3K/AKT pathways, (16, 25) providing a possible mechanism for the development of resistance to radiotherapy in malignant glioma. Our data showed that pretreatment with PP2 decreased the expression of MMP2 in glioma cells, suggesting possible mechanism of action regarding migratory inhibition of PP2 in glioma cells.

Erythropoietin-producing human hepatocellular carcinoma (Eph) receptors constitute the largest family of RTKs in the human genome. (26) In general, Eph receptors influence normal development of brain vasculature and affect brain function, including regulation of synaptic structure. Eph receptors are subdivided into EphA and EphB subgroups on the basis of sequence homology and ligand-binding specificity. Among these, EphA2 is highly overexpressed in several carcinomas including breast, gastric, and prostate cancer and is a novel target for anti-cancer therapy. The relationship between EphA2 expression and proliferative activity of gliomas has been demonstrated by several authors. (27, 28) Up-regulation of EphA2 promotes angiogenesis in brain tumors and correlates with poor prognosis of malignant gliomas. (29-32) Zhuang et al. reported that in breast cancer, EphA2 related to Trastuzumab resistance is regulated by SRC tyrosine kinase. (33) In contrast, in T-cell lymphoma, EphA2 activation leads to phosphorylation of SFK and PI3K activation. (34) In this study, EphA2 was down-regulated in U251 cells by PP2 treatment. Taken together, these findings suggest a possibility of crosstalk between SRC tyrosine kinase and EphA2 in cancer cells. However, the expression of EphA2

was not suppressed by PP2 in *in vivo* brain tumors, thus further study elucidating the mechanism is warranted.

Drawback of this study is in failure to observe statistical difference in tumor volume decrease between TMZ only and combination treatment with TMZ and PP2. This may have derived from both dramatic volume decrease of TMZ-treated tumors and small sample size of mice. As shown in Figure 7, visual response of tumors in combination treatment group was best, resulting in non-visualization of brain tumors. An addition of PP2 to TMZ showed a trend toward volume decrease.

In this study, the effect of chemoradiotherapy with SRC TKI, PP2 and TMZ in U251 cells are reported. These data show that adding PP2 to TMZ leads to additive cytotoxicity of U251 cells and decreased migration and invasion ability of U251 cells. Delayed DSBs repair after radiotherapy was demonstrated when PP2 was treated. The underlying mechanism appears to involve suppression of MMP2, which might restore sensitivity to radiotherapy and overexpression of E-cadherin, which might affect cell-to-cell adhesion. Moreover, PP2 is related to suppression of VEGF, CD31 and EphA2. These data provide evidence for combined chemoradiotherapy with TMZ and SRC TKI, PP2 on glioma cells and present a feasible strategy to improve the therapeutic outcome in malignant gliomas.

References

1. Jansen M, Yip S, Louis DN. Molecular pathology in adult gliomas: diagnostic, prognostic, and predictive markers. *Lancet Neurol* 2010;9:717-726.
2. Masui K, Cloughesy TF, Mischel PS. Review: molecular pathology in adult high-grade gliomas: from molecular diagnostics to target therapies. *Neuropathol Appl Neurobiol* 2012;38:271-291.
3. Hegi ME, Diserens AC, Gorlia T, *et al.* MGMT gene silencing and benefit from temozolomide in glioblastoma. *N Engl J Med* 2005;352:997-1003.
4. Baselga J, Cortes J, Kim SB, *et al.* Pertuzumab plus trastuzumab plus docetaxel for metastatic breast cancer. *N Engl J Med* 2012;366:109-119.
5. Blackwell KL, Burstein HJ, Storniolo AM, *et al.* Overall survival benefit with lapatinib in combination with trastuzumab for patients with human epidermal growth factor receptor 2-positive metastatic breast cancer: final results from the EGF104900 Study. *J Clin Oncol* 2012;30:2585-2592.
6. Gruber Filbin M, Dabral SK, Pazyra-Murphy MF, *et al.* Coordinate activation of Shh and PI3K signaling in PTEN-deficient glioblastoma: new therapeutic opportunities. *Nat Med* 2013;19:1518-1523.
7. Wu YL, Lee JS, Thongprasert S, *et al.* Intercalated combination of chemotherapy and erlotinib for patients with advanced stage non-small-cell lung cancer (FASTACT-2): a randomised, double-blind trial. *Lancet Oncol* 2013;14:777-786.
8. Minniti G, Amelio D, Amichetti M, *et al.* Patterns of failure and comparison of different target volume delineations in patients with glioblastoma treated with conformal radiotherapy plus concomitant and adjuvant temozolomide. *Radiother Oncol* 2010;97:377-381.
9. Angers-Loustau A, Hering R, Werbowetski TE, *et al.* SRC regulates actin dynamics and invasion of malignant glial cells in three dimensions. *Mol Cancer Res* 2004;2:595-605.
10. Stehelin D, Fujita DJ, Padgett T, *et al.* Detection and enumeration of transformation-defective strains of avian sarcoma virus with molecular hybridization. *Virology* 1977;76:675-684.

11. Stettner MR, Wang W, Nabors LB, *et al.* Lyn kinase activity is the predominant cellular SRC kinase activity in glioblastoma tumor cells. *Cancer Res* 2005;65:5535-5543.
12. Du J, Bernasconi P, Clauser KR, *et al.* Bead-based profiling of tyrosine kinase phosphorylation identifies SRC as a potential target for glioblastoma therapy. *Nat Biotechnol* 2009;27:77-83.
13. Ding Q, Stewart J, Jr., Olman MA, *et al.* The pattern of enhancement of Src kinase activity on platelet-derived growth factor stimulation of glioblastoma cells is affected by the integrin engaged. *J Biol Chem* 2003;278:39882-39891.
14. Jallal H, Valentino ML, Chen G, *et al.* A Src/Abl kinase inhibitor, SKI-606, blocks breast cancer invasion, growth, and metastasis in vitro and in vivo. *Cancer Res* 2007;67:1580-1588.
15. Buettner R, Mesa T, Vultur A, *et al.* Inhibition of Src family kinases with dasatinib blocks migration and invasion of human melanoma cells. *Mol Cancer Res* 2008;6:1766-1774.
16. Park CM, Park MJ, Kwak HJ, *et al.* Ionizing radiation enhances matrix metalloproteinase-2 secretion and invasion of glioma cells through Src/epidermal growth factor receptor-mediated p38/Akt and phosphatidylinositol 3-kinase/Akt signaling pathways. *Cancer Res* 2006;66:8511-8519.
17. Rothschild SI, Gautschi O, Haura EB, *et al.* Src inhibitors in lung cancer: current status and future directions. *Clin Lung Cancer* 2010;11:238-242.
18. Cuneo KC, Geng L, Tan J, *et al.* SRC family kinase inhibitor SU6656 enhances antiangiogenic effect of irradiation. *Int J Radiat Oncol Biol Phys* 2006;64:1197-1203.
19. Hanke JH, Gardner JP, Dow RL, *et al.* Discovery of a novel, potent, and Src family-selective tyrosine kinase inhibitor. Study of Lck- and FynT-dependent T cell activation. *J Biol Chem* 1996;271:695-701.
20. Lund CV, Nguyen MT, Owens GC, *et al.* Reduced glioma infiltration in Src-deficient mice. *J Neurooncol* 2006;78:19-29.
21. Hanson JA, Hsu FP, Jacob AT, *et al.* Antivascular endothelial growth factor antibody for treatment of glioblastoma multiforme. *Perm J* 2013;17:68-74.
22. Wong ET, Gautam S, Malchow C, *et al.* Bevacizumab for recurrent glioblastoma

- multiforme: a meta-analysis. *J Natl Compr Canc Netw* 2011;9:403-407.
23. Huvelde D, Lewis-Tuffin LJ, Carlson BL, *et al.* Targeting Src family kinases inhibits bevacizumab-induced glioma cell invasion. *PLoS ONE* 2013;8:e56505.
 24. Le DM, Besson A, Fogg DK, *et al.* Exploitation of astrocytes by glioma cells to facilitate invasiveness: a mechanism involving matrix metalloproteinase-2 and the urokinase-type plasminogen activator-plasmin cascade. *J Neurosci* 2003;23:4034-4043.
 25. Badiga AV, Chetty C, Kesanakurti D, *et al.* MMP-2 siRNA inhibits radiation-enhanced invasiveness in glioma cells. *PLoS ONE* 2011;6:e20614.
 26. Wilkinson DG. Multiple roles of EPH receptors and ephrins in neural development. *Nat Rev Neurosci* 2001;2:155-164.
 27. Wykosky J, Gibo DM, Stanton C, *et al.* EphA2 as a novel molecular marker and target in glioblastoma multiforme. *Mol Cancer Res* 2005;3:541-551.
 28. Liu F, Park PJ, Lai W, *et al.* A genome-wide screen reveals functional gene clusters in the cancer genome and identifies EphA2 as a mitogen in glioblastoma. *Cancer Res* 2006;66:10815-10823.
 29. Li X, Wang L, Gu JW, *et al.* Up-regulation of EphA2 and down-regulation of EphrinA1 are associated with the aggressive phenotype and poor prognosis of malignant glioma. *Tumour Biol* 2010;31:477-488.
 30. Wang LF, Fokas E, Bieker M, *et al.* Increased expression of EphA2 correlates with adverse outcome in primary and recurrent glioblastoma multiforme patients. *Oncol Rep* 2008;19:151-156.
 31. Zhou N, Zhao WD, Liu DX, *et al.* Inactivation of EphA2 promotes tight junction formation and impairs angiogenesis in brain endothelial cells. *Microvasc Res* 2011;82:113-121.
 32. Mosch B, Reissenweber B, Neuber C, *et al.* Eph receptors and ephrin ligands: important players in angiogenesis and tumor angiogenesis. *J Oncol* 2010;2010:135285.
 33. Zhuang G, Brantley-Sieders DM, Vaught D, *et al.* Elevation of receptor tyrosine kinase EphA2 mediates resistance to trastuzumab therapy. *Cancer Res* 2010;70:299-308.
 34. Holen HL, Shadidi M, Narvhus K, *et al.* Signaling through ephrin-A ligand leads to activation of Src-family kinases, Akt phosphorylation, and inhibition of antigen

receptor-induced apoptosis. *J Leukoc Biol* 2008;84:1183-1191.

국문초록

SRC 티로신 인산화효소 억제제인 PP2와 테모졸로마이드 병용치료의 악성 교종 세포에 대한 *in vitro* 및 *in vivo* 효과

서론: 교모세포종에서 SRC 티로신 인산화효소의 과발현은 종양의 악성도 및 치료에 대한 좋지 않은 예후와 연관되어있다. 테모졸로마이드(TMZ)와 SRC 티로신 인산화효소 억제제인 PP2를 병용치료하는 것이 종양세포의 성장과 침윤을 억제하여 방사선치료의 치료율을 높일 수 있는지 집락형성분석법과 누드마우스를 이용한 뇌종양 이식모델을 이용하여 평가하였다.

방법: U251과 T98G 세포주에 SRC 티로신 인산화효소 억제제인 PP2(10 μ M)와 TMZ(25 μ M)를 처리하여 집락형성분석법을 이용한 방사선 감작을 조사하였다. PP2를 방사선 조사 전에 전처리하는 것이 DNA 이중나선 손상의 수복을 저해하는가에 대해 방사선조사 6시간 후에 γ H2AX 형성 분석을 이용하여 평가하였다. PP2가 U251 세포주의 이동이나 침윤에 영향을 미치는가에 대해서 변형보이든합분석과 상처치유분석을 이용하여 평가하였고, 혈관유사형성 측정을 수행하였다. E-cadherin, MMP2, EphA2 및 VEGF의 단백질 발현을 평가하기 위해서 웨스턴블롯검사를 하였다. 뇌종양 이식모델에서는 3×10^5 개의 U251 세포주를 누드마우스의 시상 부위에 이식하고 PP2(10mg/kg)와 TMZ(50mg/kg)를 전뇌방사선(9Gy/3Fx) 치료 전, 치료 중간 및 치료 후에 처리하였다. pGL4 루시퍼레이스 정보제공 벡터를 이용하여 생물발광 영상을 얻어서 마우스 내의 종양의 부피를 측정하였다. 또한 뇌종양에 대한 VEGF, CD31, EphA2와 HIF-1 α 에 대한 면역화학염색을 시행하였다.

결과: PP2를 전처리하는 것은 정상적인 인간 별아교세포에는 명확한 세포독성 없이 방사선치료 후 U251 세포주의 세포독성을 증가시키고 생존분획을 감소시켰다. 생존분획이 0.5일 때 PP2, TMZ, PP2 및 TMZ를 병용처리했을 때의 민감제 증강률은 U251 세포주에서 각각 1.15, 1.41 및 1.54였으며, T98G 세포주에서는 1.16, 1.26 및 1.38였다. PP2를 처리한 경우 U251 세포주의 침윤 및 이동 능력이 떨어졌다. 방사선 단독조사에

비해서 억제제를 처리한 세포들의 상대적 이동 능력은 PP2, TMZ, PP2 와 TMZ를 병용처리했을 때 각각 0.993 ± 0.131 ($p = 0.465$), 0.252 ± 0.078 ($p < 0.001$) 및 0.200 ± 0.066 ($p < 0.001$)였다. 억제제를 처리한 세포들의 상대적 침윤 능력은 방사선 단독조사에 비해서 PP2, TMZ, PP2 와 TMZ를 병용처리했을 때 각각 0.992 ± 0.122 ($p = 0.461$), 0.257 ± 0.050 ($p < 0.001$) 및 0.116 ± 0.010 ($p < 0.001$)였다. PP2에 의해 U251 세포주의 혈관유사형성이 억제되었다. PP2를 처리하였을 때 E-cadherin이 과발현되고 MMP2와 VEGF 및 EphA2는 억제되었다. PP2와 TMZ를 병용처리했을 때 방사선치료 6시간 후 γ H2AX 초점의 축적이 증가했으며 이러한 결과는 DNA 손상의 수복이 지연됨을 의미하였다.

뇌종양 이식모델에서는 TMZ와 PP2를 병용치료할 때 종양의 부피가 가장 많이 줄었으나 TMZ 단독치료와 비교할 때에 통계적 차이는 없었다. PP2를 처리한 종양에서 방사선 단독치료 또는 방사선과 TMZ 치료를 한 종양에 비해 VEGF와 CD31의 발현이 억제되었다. 이러한 결과는 PP2가 세포실험과 마찬가지로 동물 내 종양에서도 혈관신생을 억제할 수 있음을 시사하였다. EphA2와 HIF-1 α 의 발현은 PP2 치료에 의해 억제되지 않았다.

결론: SRC 티로신 인산화효소를 억제할 경우 방사선치료에 의한 세포독성이 증가하고 이러한 효과는 MGMT 프로모터의 메틸화와는 무관하였다. 또한 PP2는 U251 세포주의 침윤, 이동 및 혈관유사형성을 억제하였다. PP2는 뇌종양 이식모델에서 VEGF와 CD31의 발현을 억제하여 항혈관신생효과에 대한 가능성을 보였다. 이러한 실험결과는 TMZ와 SRC 티로신 인산화효소 억제제인 PP2를 병용치료하는 것에 대한 실험증거를 제공하며, 이러한 치료가 악성 교종에서 치료효과를 향상시킬 수 있는 가능한 전략임을 나타낸다.

주요어: SRC 티로신 인산화효소 억제제, PP2, 교모세포종, 악성교종, 병용치료, 방사선치료

학 번: 2008-30529